

NCN Pincer–Pt Complexes Coordinated by (Nitronyl Nitroxide)-2-ide Radical Anion

Xun Zhang, Shuichi Suzuki, Masatoshi Kozaki, and Keiji Okada*

Department of Chemistry, Graduate School of Science, Osaka City University, Sumiyoshi-ku, Osaka 558-8585, Japan

Supporting Information

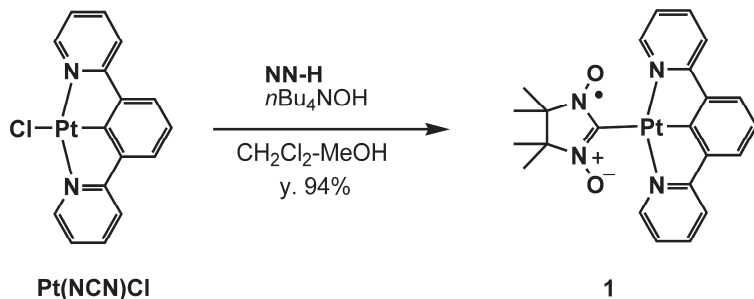
1. General methods and synthetic procedures pp. S2–S6.
2. Figure S1. Crystal structures of **2**. p. S7
3. Figure S2. Crystal structures of **1** with H₂O or EtOH. p. S8
4. Figure S3. Absorption spectra of **1** in CH₂Cl₂–MeOH p. S9
5. Density functional theory calculations for **1**. pp. S9–S14
6. Figure S4. ESR spectra for **2** and **3**. p. S15
7. Figure S5. Crystal structures of **1**⁺ involving two structurally independent molecules. p. S16
8. Figure S6. ¹H NMR spectrum of **1**⁺. pp. S17–S19
9. Figure S7. HMQC and HMBC spectra of **1**⁺. pp. S20–S22

General methods:

Chemicals were of commercial grade and used without further purification. Dichloromethane and acetonitrile were dried and distilled over calcium hydride. Methanol and ethanol were dried and distilled over magnesium.

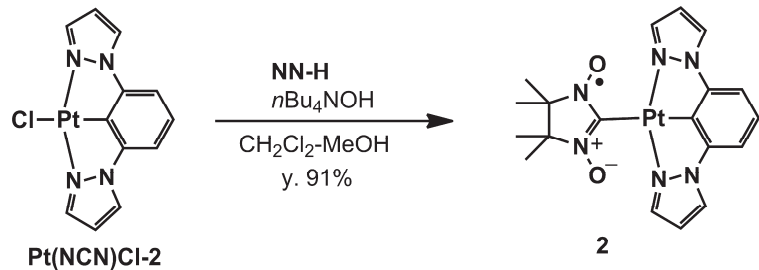
^1H NMR spectra were recorded on a BRUKER AVANCE 600 spectrometer. FAB-MS spectra were recorded on a JEOL JMS-AX-500 spectrometer. Melting points were measured using a Yanako MP-J3 apparatus, and are not corrected. Infrared spectra were measured using a Shimadzu FT-IR-8700 spectrometer. ESR spectra were recorded on a Bruker ELEXSYS E500 spectrometer. Redox potentials were measured using ALS Electrochemical analyzer MODEL 610A in a conventional three-electrode cell equipped with a glassy carbon as a working electrode, a platinum wire as a counter electrode, and a saturated calomel electrode (SCE) as a reference electrode. The measurements were carried out with a sweep rate of 100 mV/s in dichloromethane containing 0.1 M tetra-*n*-butylammonium perchlorate as an electrolyte. The redox potentials were finally corrected by a ferrocene/ferrocenium couple (Fc/Fc^+). Absorption spectra were measured on JASCO V-750. X-ray data were collected by a Rigaku CCD detector with graphite monochromated Mo-K α radiation.

Preparation of compound 1.



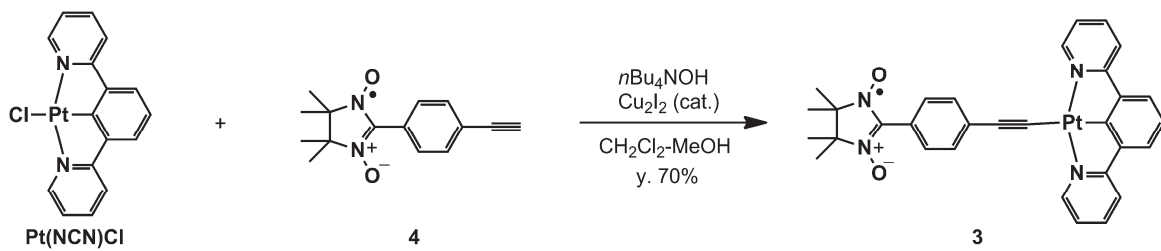
4,4,5,5-Tetramethylimidazoline-3-oxide-1-oxyl (**NN-H**) (50.0 mg, 0.32 mmol) and **Pt(NCN)Cl^{S1}** (147.4 mg, 0.32 mmol) were dissolved in a mixture of dichloromethane (5 mL) and methanol (5 mL) under nitrogen. A methanol solution of tetrabutylammonium hydroxide (37%, 0.5 mL) was added dropwise to this solution at room temperature. The mixture was further stirred for 1 h and poured into water. The whole mixture was transferred into a separatory funnel containing dichloromethane (20 mL). The organic layer was washed with water, dried over anhydrous sodium sulfate, filtered, and concentrated under reduced pressure. The residue was recrystallized from dichloromethane–ethanol, to give **1** as a purple solid (176 mg, 94%). Crystals suitable for X-ray crystal structure analysis were obtained by recrystallization from dichloromethane–methanol. **1**: mp 247 °C (decomp.). IR (KBr, cm⁻¹): 3024, 2974, 1608, 1579, 1489, 1469, 1448, 1286, 1205, 1134, 1087, 1035, 877, 843, 769, 540. MS (FSB⁺) *m/z* 583 [M⁺ + H]. Anal. Calcd. for C₂₃H₂₃N₄O₂Pt·CH₃OH: C, 46.90; H, 4.43; N, 9.12. Found: C, 46.57; H, 4.42; N, 8.98. ESR (in CH₂Cl₂ at room temperature): *g* = 2.0062 (*v*₀ = 9.443659 GHz), |*a*_{Pt}| = 1.655 mT, |*a*_N| = 0.811 mT.

Preparation of compound 2.



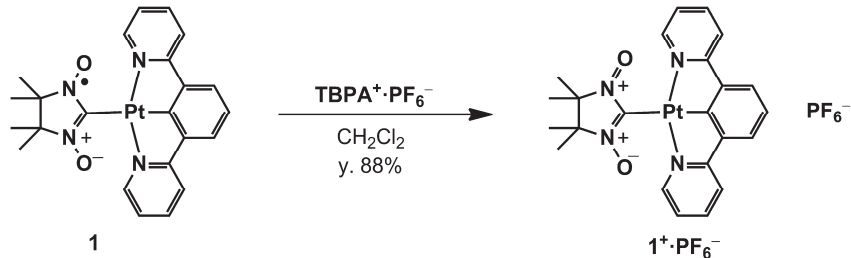
4,4,5,5-Tetramethylimidazoline-3-oxide-1-oxyl (**NN-H**) (31 mg, 0.20 mmol) and **Pt(NCN)Cl-2^{S2}** (87 mg, 0.20 mmol) were dissolved in dichloromethane (1 mL) under nitrogen. A methanol solution of tetrabutylammonium hydroxide (37%, 0.5 mL) was added dropwise to this solution at room temperature. The mixture was stirred for 24 h and poured into water. The whole mixture was transferred in a separatory funnel containing dichloromethane (20 mL). The organic layer was separated, washed with water, dried over anhydrous sodium sulfate, filtered, and concentrated under reduced pressure, to give almost pure **2** (102 mg, 91%). The crystals suitable for X-ray crystal structure analysis were obtained by recrystallization from dichloromethane. **2**: mp 215 °C (decomp.). IR (KBr, cm^{-1}): 3089, 2985, 2925, 1603, 1516, 1498, 1471, 1413, 1326, 1290, 1209, 1136, 1051, 1029, 981, 824, 773, 758, 746, 603, 540. MS (FAB⁺) m/z 561 [M⁺ + H]. Anal. Calcd. for $\text{C}_{19}\text{H}_{21}\text{N}_6\text{O}_2\text{Pt} \cdot 0.4\text{C}_8\text{H}_{10}(p\text{-xylene}) \cdot 0.1\text{CH}_2\text{Cl}_2$ recrystallized from *p*-xylene–dichloromethane: C, 43.80; H, 4.15; N, 13.74. Found: C, 43.72; H, 4.03; N, 13.48. ESR (in CH_2Cl_2 at room temperature): $g = 2.0066$ ($\nu_0 = 9.446656$ GHz), $|a_{\text{Pt}}| = 1.655$ mT, $|a_{\text{N}}| = 0.811$ mT.

Synthesis of compound 3.



Compound **4**^{S3} (51 mg, 0.20 mmol) and **Pt(NCN)Cl** (92 mg, 0.20 mmol) were dissolved in dichloromethane (3 mL) under nitrogen in the presence of copper(I) iodide (3 mg). A methanol solution of tetrabutylammonium hydroxide (37%, 0.3 mL) was added dropwise to this solution at room temperature and the mixture was further stirred for 1 h. Then, the reaction mixture was poured into water in a separatory funnel. Dichloromethane was added to the separatory funnel. The organic layer was separated, washed with water, dried over anhydrous sodium sulfate, filtered, and concentrated under reduced pressure, to give **3** (96 mg, 70%). We could not find out a good recrystallization solvent for this compound. The following data are those without further purification. **3**: mp 82 °C (decomp.). IR (KBr, cm⁻¹): 3394, 2960, 2081, 1606, 1485, 1467, 1446, 1419, 1388, 1355, 1298, 1215, 1164, 1132, 837, 767, 542. MS (FSB⁺) *m/z* 682 [M⁺ + H]. High resolution MS (FAB⁺): found *m/z* 682.1783. calcd for C₃₁H₂₇N₄O₂Pt *m/z* 682.1782. ESR (in CH₂Cl₂ at room temperature): *g* = 2.0065 (*v*₀ = 9.43660 GHz), |*a*_N| = 0.756 mT.

Synthesis of $\mathbf{1}^+\cdot\text{PF}_6^-$



In a glove box filled with argon, compound **1** (106 mg, 0.18 mmol) was dissolved in dichloromethane (20 mL). To this stirred solution of **1**, was added a dichloromethane solution (20 mL) of tris(4-bromophenyl)aminium hexafluorophosphate ($\text{TBPA}^+\cdot\text{PF}_6^-$) (116 mg, 0.18 mmol). Precipitates appeared during the addition of $\text{TBPA}^+\cdot\text{PF}_6^-$. After 30 min, the precipitates were collected by filtration to give $\mathbf{1}^+\cdot\text{PF}_6^-$ as a brown solid (117 mg, 88%). The crystalline solid was obtained by recrystallization from $\text{CH}_2\text{Cl}_2\text{-Et}_2\text{O}$. $\mathbf{1}^+\cdot\text{PF}_6^-$: mp >300 °C (decomp.). IR (KBr, cm^{-1}) 2997, 1610, 1595, 1488, 1469, 1421, 1380, 1182, 1130, 840, 761, 557. MS (FAB $^+$) m/z 583 [NN $^+$ -Pt(NCN)-**1** + H], (FAB $^-$) m/z 145 (PF_6^-). ^1H NMR (600 MHz, CD_2Cl_2): δ 8.04 (ddd, $J = 7.7, 7.7, 1.4$ Hz, 2H), 7.81 (dd, $J = 7.7, 1.4$ Hz, 2H), 7.67 (ddd, $J = 42.1$ ($^3J_{\text{PtH}}$), 5.7, 1.4 Hz, 2H), 7.59 (d, $J = 7.8$ Hz, 2H), 7.35 (d, $J = 7.8$ Hz, 1H), 7.21 (ddd, $J = 7.7, 5.7, 1.4$ Hz, 2H), 1.83 (s, 12H). Anal. Calcd. for $\text{C}_{23}\text{H}_{23}\text{F}_6\text{N}_4\text{O}_2\text{PPt}$: C, 37.97; H, 3.19; N, 7.70. Found: C, 38.09; H, 3.26; N, 7.65.

References

- (S1) Cárdenas, D. J.; Echavarren, A. M. *Organometallics* **1999**, *18*, 3337–3341.
- (S2) Willison, S. A.; Krause, J. A.; Connick, W. B. *Inorg. Chem.* **2008**, *47*, 1258–1260.
- (S3) Klyatskaya, S. V.; Tretyakov, E. V.; Vasilevsky, S. F. *Russ. Chem. Bull.* **2002**, *51*, 128–134.

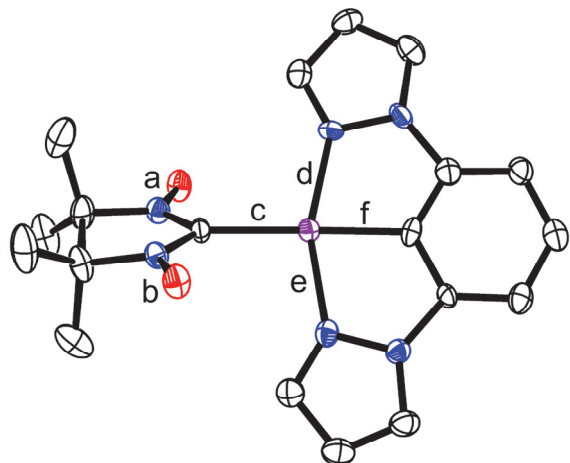


Figure S1. Crystal structures of **2** drawn at a 50% ellipsoid level measured at 150 K: Selected bond lengths (\AA): **a** (N–O): 1.312, **b** (N–O): 1.301, **c** (Pt–C): 2.062, **d** (Pt–N): 2.022, **e** (Pt–N): 2.028, **f** (Pt–C): 1.948. Hydrogen atoms and the solvent molecule (CH_2Cl_2) involved in the crystal are omitted for clarity.

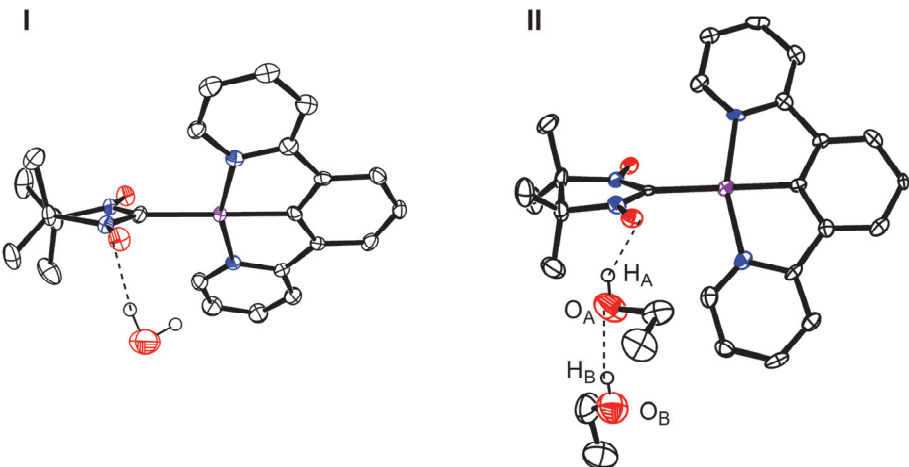


Figure S2. Crystal structures of **1** with hydrogen bonded water (**I**)^{S4} and with ethanol (**II**)^{S5} (drawn at a 50% ellipsoid level measured at 150 K): Hydrogen bond lengths (Å) in **I**: (H—O(NO)) = 1.806, ((H₂O)O—O(NO)) = 2.797; in **II**: (H_A—O(NO)) = 1.903, (O_A—O(NO)) = 2.670, (H_B—O_A) = 2.013, (O_B—O_A) = 2.839.

References.

- (S4) Crystallographic data of **1** with hydrogen bonded H₂O: monoclinic, space group: *P2₁/n* (#14), $a = 9.9464(14)$, $b = 15.361(2)$, $c = 14.300(2)$ Å, $\beta = 97.978(3)^\circ$, $V = 2163.7(5)$ Å³, $Z = 4$, $\rho_{\text{calc}} = 1.844$ g cm⁻³, $T = 200(2)$ K, $R = 0.0425$, $wR = 0.0743$, GOF = 1.270 (CCDC#: 859135).
- (S5) Crystallographic data of **1** with hydrogen bonded EtOH: triclinic, space group: *P-1* (#2), $a = 8.8562(13)$, $b = 10.4837(19)$, $c = 16.091(3)$ Å, $\alpha = 81.251(17)^\circ$, $\beta = 75.385(17)^\circ$, $\gamma = 66.316(13)^\circ$, $V = 1321.7(4)$ Å³, $Z = 2$, $\rho_{\text{calc}} = 1.695$ g cm⁻³, $T = 120(2)$ K, $R = 0.0601$, $wR = 0.1226$, GOF = 1.090 (CCDC#: 859136).

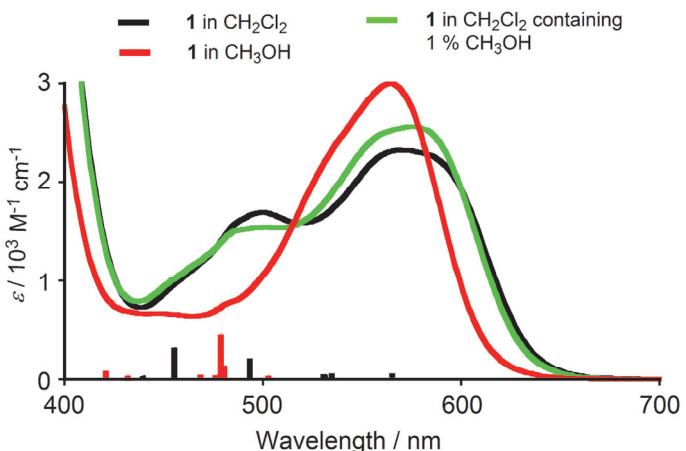


Figure S3. Absorption spectra of **1** in CH_2Cl_2 (black line), in CH_2Cl_2 containing 1% of CH_3OH (green line), and in CH_3OH (red line). The small bars (black for free **1**, red for **1** with hydrogen-bonded CH_3OH) on the wavelength axis stand for the relative values of oscillator strength obtained by TDDFT/UB3PW91 calculations (see the section of Density functional theory calculations for **1**). The calculations qualitatively account for the relative sequence of energies of absorptions and number of the major peaks, although the calculated energies were considerably higher than the observed energies in all transitions.

Density functional theory calculations for **1:** DFT calculations were carried out at the B3PW91 level.^{S6} Basis sets employed were 6-31G(d) for C, H, O, and N, atoms and Hay-Wadt double-zeta functions with Los Alamos relativistic effective core potential (LANL2DZ) for Pt atom.^{S7} All calculations were performed with the GAUSSIAN 09 Revision A.02.^{S8} TDDFT calculations of **1** with hydrogen bonded methanol were performed at the geometry of the crystal structure (Figure 2a in the text), whereas the calculations of free **1** were achieved at the same geometry without CH_3OH . The results of TDDFT calculations are shortly summarized as follows:

TDDFT calculation for free 1 (A-Orbital: HOMO 112A; LUMO113A, B-Orbital: HOMO 111B; 112B):

Excitation energies and oscillator strengths:

Excited State 1: 2.041-A 1.4960 eV 828.79 nm f=0.0001
 $\langle S^{**2} \rangle = 0.791$
112A ->113A 0.95518
112A ->114A -0.28529

This state for optimization and/or second-order correction.

Copying the excited state density for this state as the 1-particle RhoCI density.

Excited State 2: 2.045-A 1.6242 eV 763.34 nm f=0.0000
 $\langle S^{**2} \rangle = 0.795$
112A ->113A 0.28607
112A ->114A 0.95672

Excited State 3: 2.872-A 2.1934 eV 565.26 nm f=0.0020
 $\langle S^{**2} \rangle = 1.812$
111B ->112B 0.90342
111B ->113B -0.40816

Excited State 4: 2.887-A 2.3137 eV 535.87 nm f=0.0032
 $\langle S^{**2} \rangle = 1.833$
111B ->112B 0.40788
111B ->113B 0.89933

Excited State 5: 2.054-A 2.3288 eV 532.40 nm f=0.0022
 $\langle S^{**2} \rangle = 0.805$
112A ->115A 0.99400

Excited State 6: 2.022-A 2.5094 eV 494.09 nm f=0.0143
 $\langle S^{**2} \rangle = 0.772$
112A ->116A 0.79041
112A ->120A -0.20106
112A ->121A -0.11179
111B ->114B -0.43309
111B ->115B -0.32423

Excited State 7: 3.440-A 2.6538 eV 467.19 nm f=0.0001
 $\langle S^{**2} \rangle = 2.709$
105A ->114A -0.21411
106A ->114A 0.12903
107A ->113A 0.15597
107A ->114A 0.36959
108A ->113A -0.19141
109A ->114A 0.10154
110A ->113A -0.11837

111A ->113A	-0.35151
111A ->114A	0.17924
111A ->116A	-0.11238
105B ->112B	0.11490
105B ->113B	0.20571
106B ->112B	-0.15816
106B ->113B	-0.24777
107B ->112B	0.16480
107B ->113B	0.26493
108B ->112B	0.32769
108B ->113B	-0.20060
108B ->116B	0.12515
108B ->117B	0.10161

Excited State 8: 2.089-A 2.6603 eV 466.05 nm f=0.0003
 $\langle S^{**2} \rangle = 0.841$

109B ->114B	0.12659
109B ->115B	0.12339
110B ->114B	0.69424
110B ->115B	0.64855

Excited State 9: 2.077-A 2.7189 eV 456.01 nm f=0.0224
 $\langle S^{**2} \rangle = 0.829$

112A ->116A	0.59800
112A ->117A	-0.14328
112A ->120A	0.25325
112A ->121A	0.15131
111B ->114B	0.63130
111B ->115B	0.32136

Excited State 10: 3.382-A 2.8176 eV 440.04 nm f=0.0018
 $\langle S^{**2} \rangle = 2.610$

107A ->113A	-0.22174
107A ->114A	0.13620
108A ->113A	0.15336
108A ->114A	0.19535
110A ->114A	0.15089
111A ->113A	0.23669
111A ->114A	0.52320
106B ->112B	0.16575
107B ->112B	-0.15908
108B ->112B	-0.27633
108B ->113B	-0.46654
111B ->113B	0.10811
111B ->115B	0.12449

SavETr: write IOETrn= 770 NScale= 10 NData= 16 NLR=1 LETran= 190.

TDDFT calculation for 1 with hydrogen bonded CH₃OH (A-Orbital: HOMO 121A; LUMO122A, B-Orbital: HOMO 120B; 121B)

Excitation energies and oscillator strengths:

Excited State 1: 2.037-A 1.8050 eV 686.88 nm f=0.0002
 $\langle S^{**2} \rangle = 0.787$

121A ->122A 0.98085
121A ->123A -0.16436

This state for optimization and/or second-order correction.

Copying the excited state density for this state as the 1-particle RhoCI density.

Excited State 2: 2.040-A 1.9516 eV 635.30 nm f=0.0001
 $\langle S^{**2} \rangle = 0.790$

121A ->122A 0.16564
121A ->123A 0.98466

Excited State 3: 2.951-A 2.4655 eV 502.88 nm f=0.0021
 $\langle S^{**2} \rangle = 1.927$

119A ->122A -0.14325
117B ->121B 0.13495
120B ->121B 0.92393
120B ->122B -0.23127

Excited State 4: 2.054-A 2.5774 eV 481.04 nm f=0.0091
 $\langle S^{**2} \rangle = 0.805$

121A ->125A -0.15387
121A ->128A 0.11848
116B ->123B 0.10805
117B ->123B 0.25709
118B ->123B 0.79714
118B ->124B 0.12473
119B ->123B 0.15699
120B ->123B -0.39639

Excited State 5: 2.136-A 2.5887 eV 478.95 nm f=0.0324
 $\langle S^{**2} \rangle = 0.891$

121A ->124A 0.13374
121A ->125A 0.22768
121A ->126A 0.11993
121A ->128A -0.21475
121A ->129A 0.13181
118B ->123B 0.41919
120B ->121B -0.14605
120B ->122B -0.29497
120B ->123B 0.70442

Excited State 6: 2.943-A 2.5955 eV 477.69 nm f=0.0033
 $\langle S^{**2} \rangle = 1.915$

119A ->123A -0.20335
117B ->122B 0.19491
118B ->123B 0.11763
120B ->121B 0.22095
120B ->122B 0.84889
120B ->123B 0.27062

Excited State 7: 2.085-A 2.6460 eV 468.56 nm f=0.0027
 $\langle S^{**2} \rangle = 0.837$

121A ->124A 0.97607
120B ->123B -0.10979

Excited State 8: 3.342-A 2.6749 eV 463.52 nm f=0.0003
 $\langle S^{**2} \rangle = 2.542$

113A ->123A -0.20120
116A ->122A 0.15992
116A ->123A 0.39593
118A ->123A 0.10365
119A ->122A -0.38552
119A ->125A -0.11793
121A ->124A -0.13122
113B ->122B 0.20027
114B ->122B -0.10529
115B ->121B -0.15859
115B ->122B -0.37793
116B ->122B -0.11025
117B ->121B 0.32096
117B ->125B 0.11035
120B ->121B -0.22718
120B ->122B 0.17305

Excited State 9: 3.282-A 2.8657 eV 432.65 nm f=0.0021
 $\langle S^{**2} \rangle = 2.443$

115A ->123A 0.14056
116A ->122A -0.28941
118A ->122A -0.10486
119A ->122A 0.15562
119A ->123A 0.56469
121A ->125A -0.12104
115B ->121B 0.24721
117B ->121B -0.16095
117B ->122B -0.43264
118B ->122B 0.16239
120B ->122B 0.30157

Excited State 10: 2.078-A 2.9416 eV 421.48 nm f=0.0049
 $\langle S^{**2} \rangle = 0.830$
 121A ->125A 0.93862
 120B ->123B -0.26063
 SavETr: write IOETrn= 770 NScale= 10 NData= 16 NLR=1 LETrn= 190.

- (S6) (a) Becke, A. D. *Phys. Rev. A* **1988**, *38*, 3098–3100. (b) Becke, A. D. *J. Chem. Phys.* **1993**, *98*, 5648–5652. (c) Lee, C.; Yang, W.; Parr, R. G. *Phys. Rev. B* **1988**, *37*, 785–789.
- (S7) Hay, P. J.; Wadt, W. R., *J. Chem. Phys.*, **1985**, *82*, 299–310.
- (S8) Gaussian 09, Revision A.02, Frisch, M. J.; Trucks, G. W.; Schlegel, H. B.; Scuseria, G. E.; Robb, M. A.; Cheeseman, J. R.; Scalmani, G.; Barone, V.; Mennucci, B.; Petersson, G. A.; Nakatsuji, H.; Caricato, M.; Li, X.; Hratchian, H. P.; Izmaylov, A. F.; Bloino, J.; Zheng, G.; Sonnenberg, J. L.; Hada, M.; Ehara, M.; Toyota, K.; Fukuda, R.; Hasegawa, J.; Ishida, M.; Nakajima, T.; Honda, Y.; Kitao, O.; Nakai, H.; Vreven, T.; Montgomery, Jr., J. A.; Peralta, J. E.; Ogliaro, F.; Bearpark, M.; Heyd, J. J.; Brothers, E.; Kudin, K. N.; Staroverov, V. N.; Kobayashi, R.; Normand, J.; Raghavachari, K.; Rendell, A.; Burant, J. C.; Iyengar, S. S.; Tomasi, J.; Cossi, M.; Rega, N.; Millam, J. M.; Klene, M.; Knox, J. E.; Cross, J. B.; Bakken, V.; Adamo, C.; Jaramillo, J.; Gomperts, R.; Stratmann, R. E.; Yazyev, O.; Austin, A. J.; Cammi, R.; Pomelli, C.; Ochterski, J. W.; Martin, R. L.; Morokuma, K.; Zakrzewski, V. G.; Voth, G. A.; Salvador, P.; Dannenberg, J. J.; Dapprich, S.; Daniels, A. D.; Farkas, Ö.; Foresman, J. B.; Ortiz, J. V.; Cioslowski, J.; Fox, D. J. Gaussian, Inc., Wallingford CT, 2009.

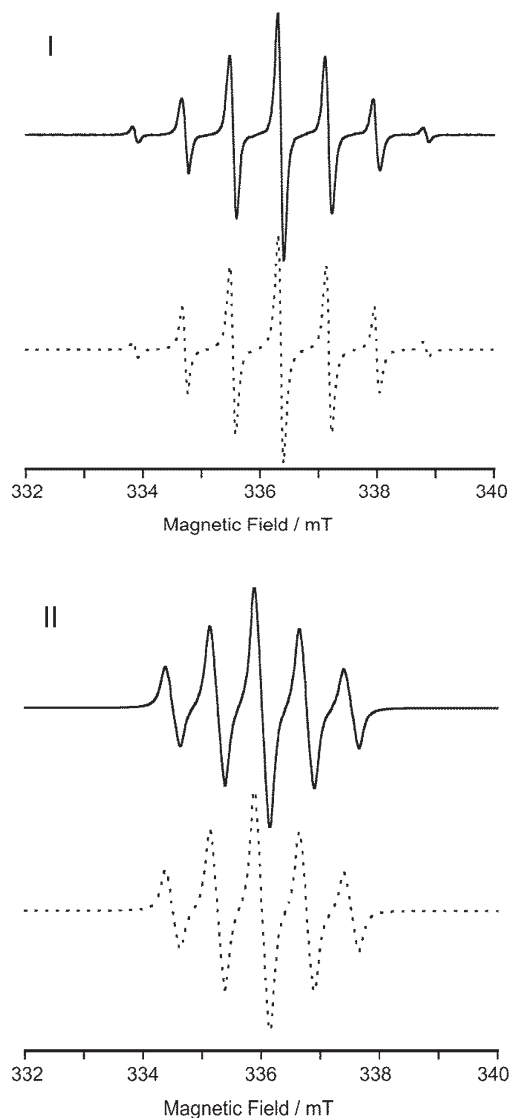


Figure S4. ESR spectra of **2** (**I**) and **3** (**II**) in dichloromethane at room temperature. The solid and dotted lines show the observed and the simulated spectra, respectively. Parameters for simulation: **I**: $g = 2.0066$ ($\nu_0 = 9.446656$ GHz), $|a_{\text{Pt}}| = 1.700$ mT, $|a_{\text{N}}| = 0.814$ mT; **II**: $g = 2.0065$ ($\nu_0 = 9.43660$ GHz), $|a_{\text{N}}| = 0.756$ mT.

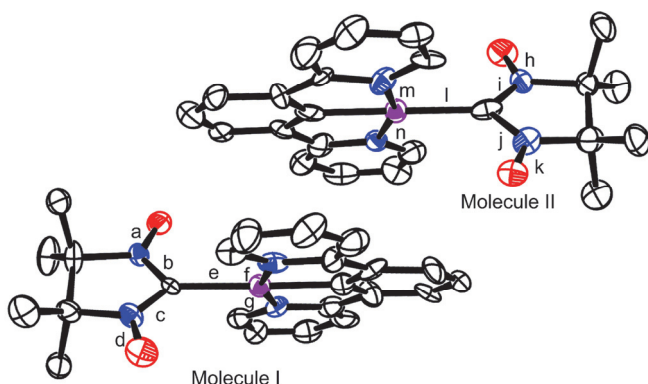


Figure S5. Crystal structures of $\mathbf{1}^+$ ($\text{NN}^+\text{-Pt}(\text{NCN})\text{-1}$) drawn at a 50% ellipsoid level measured at 150 K: Selected bond lengths (\AA) for the two independent molecules I and II: Molecule I: **a** (N–O): 1.231, **b** (C–N): 1.384, **c** (C–N): 1.346, **d** (N–O): 1.250, **e** (Pt–C): 2.073, **f** (Pt–N): 2.076, **g** (Pt–N): 2.082 \AA , Molecule II: **h** (N–O): 1.215, **i** (C–N): 1.372, **j** (C–N): 1.346, **k** (N–O): 1.270, **l** (Pt–C): 2.067, **m** (Pt–N): 2.043, **n** (Pt–N): 2.072 \AA . There were disorders in the crystalline solvent molecule (CH_2Cl_2) and the counter ions (PF_6^-), which are omitted for clarity. Hydrogen atoms are also omitted for clarity. Molecule II has slightly different N–O bond lengths (**h**: 1.215 and **k**: 1.270 \AA) and also C–N bond lengths (**i**: 1.372 and **j**: 1.346 \AA) and thus in a slightly asymmetric structure deviating to one of the canonical form of the nitrosonium nitroxide $\text{O}=\text{N}^+-\text{C}=\text{N}^+-\text{O}^-$, although the degree of asymmetry is generally small as observed in Molecule I and previously reported nitrosonium nitroxides (reference 10 and 16 in the text). The reason of the asymmetric structure may be due to asymmetric intermolecular contacts around Molecule II.

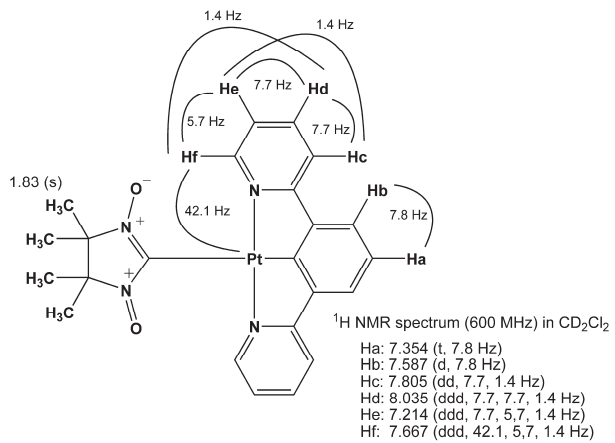
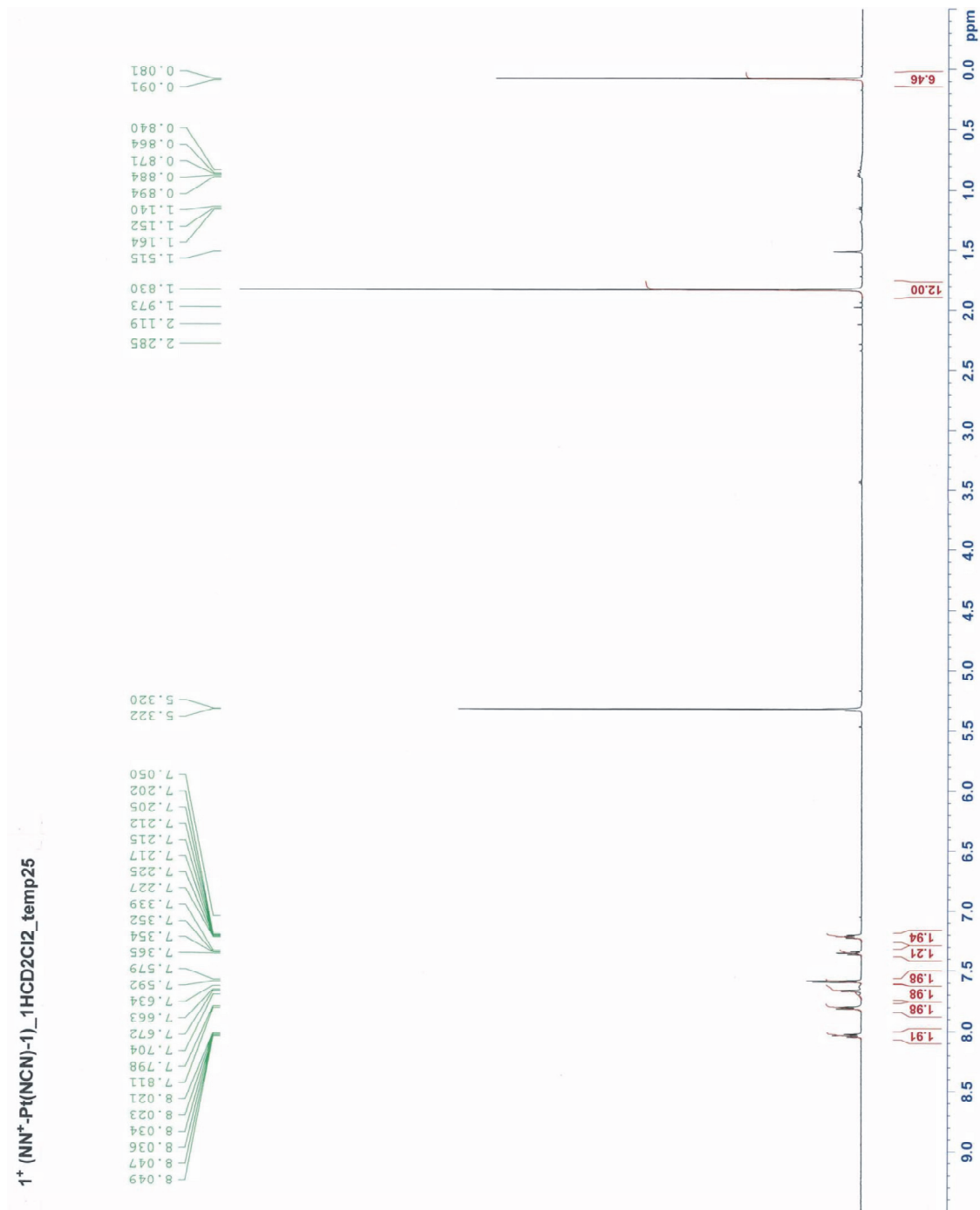
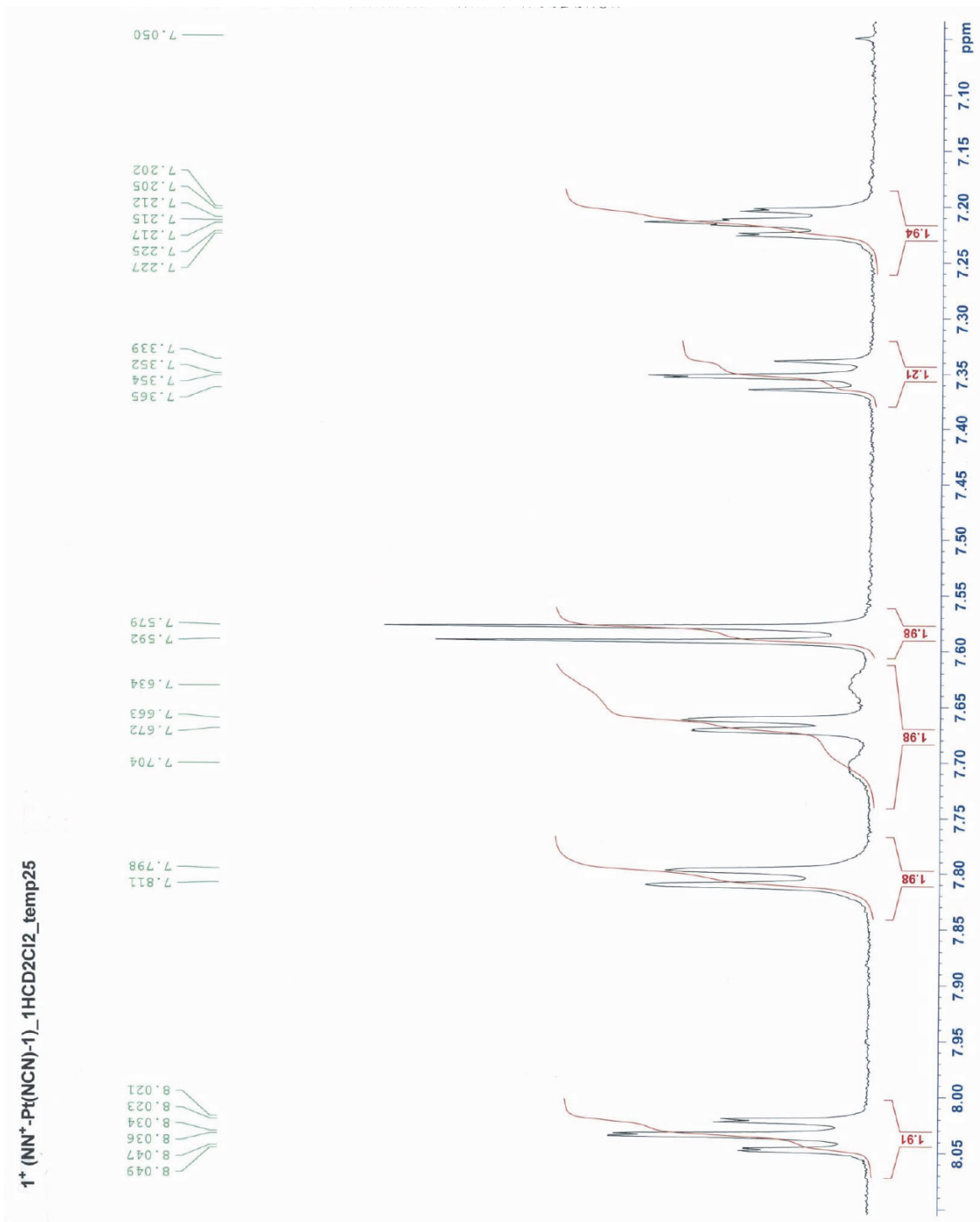


Figure S6. ¹H NMR (600 MHz in CD₂Cl₂) assignment of compound **1⁺** (**NN⁺-Pt(NCN)-1**): Ha: δ 8.35 (t, *J* = 7.8 Hz, 1H), Hb: 7.59 (d, *J* = 7.8 Hz, 2H), Hc: 7.81 (brd, *J* ~ 7.7 Hz, 2H), Hd: 8.04 (ddd, *J* = 7.7, 7.7, 1.4 Hz, 2H), He: 7.21 (ddd, 7.7, 5.7, 1.4 Hz, 2H), Hf: 7.67 (ddd, *J* = 42.1 (³*J*_{PtH}), 5.7, 1.4 Hz, 2H), methyl protons: 1.83 (s, 12H).

$1^+ (\text{NN}^+\text{-Pt(NCN)-1})\text{-1HCD2Cl}_2\text{-temp25}$





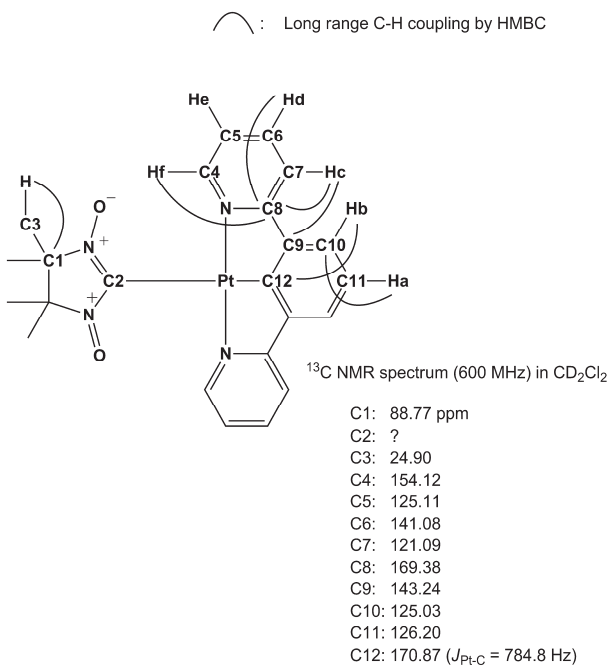
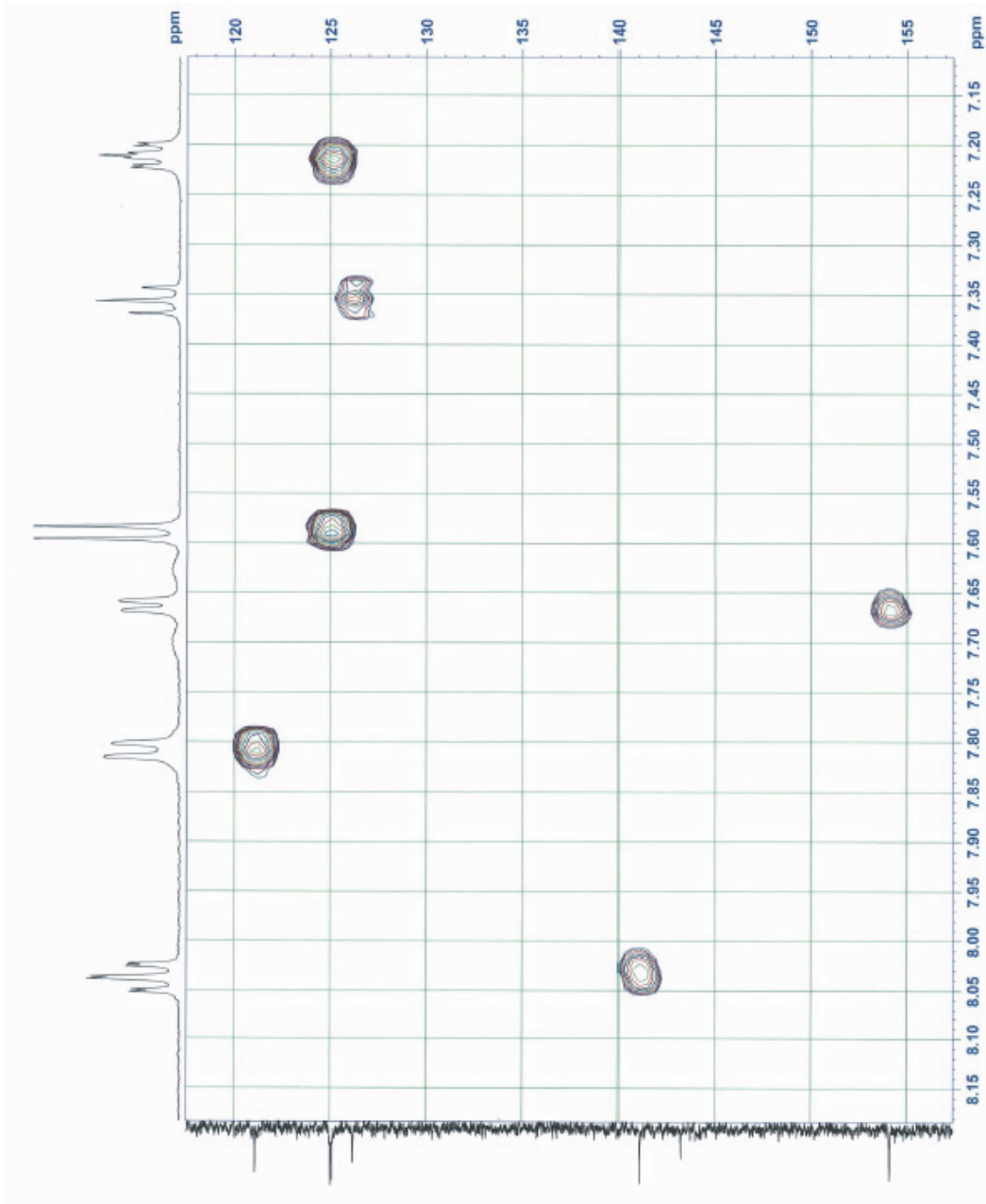


Figure S7. ^{13}C NMR (600 MHz in CD_2Cl_2) assignment of compound $\mathbf{1}^+$ ($\text{NN}^+-\text{Pt}(\text{NCN})-\mathbf{1}$): C1: 24.90, C2: 88.77, C4: 154.12, C5: 125.11, C6: 141.08, C7: 121.09, C8: 169.38, C9: 143.24, C10: 125.03, C11: 126.20, and C12: 170.87 ppm. The chemical shift of the C2 carbon atom could not be determined because of the low solubility of $\mathbf{1}^+$.

1⁺13CCD2Cl2_hmqc_temp25



1⁺13CCD2Cl₂_hmbc_temp25

